

1 **Geometric morphometrics out-perform linear-based methods in the**
2 **taxonomic resolution of a mammalian species complex**

3 Pietro Viacava^{1,2*}, Simone P. Blomberg³, Vera Weisbecker^{1,2*}

4 ¹College of Science and Engineering, Flinders University, Adelaide, South Australia, Australia

5 ²Australian Research Council Centre of Excellence for Australian Biodiversity and Heritage

6 ³School of Biological Sciences, The University of Queensland, St Lucia, Queensland, Australia

7

8

9

10

11

12

13

14

15 **Correspondence authors:** Pietro Viacava (pietroviama@hotmail.com) and
16 Vera Weisbecker (vera.weisbecker@flinders.edu.au).

17 **Running headline:** Morphometric methods for taxonomic resolution

18 **Abstract**

19 1. Morphology-based taxonomic research frequently applies linear morphometrics (LMM) in
20 skulls to quantify species distinctions. The choice of which measurements to collect
21 generally relies on the expertise of the investigators or a set of standard measurements, but
22 this practice may ignore less obvious or common discriminatory characters. In addition,
23 taxonomic analyses often ignore the potential for subgroups of an otherwise cohesive
24 population to differ in shape purely due to size differences (or allometry). Geometric
25 morphometrics (GMM) is more complicated as an acquisition technique, but can offer a more
26 holistic characterization of shape and provides a rigorous toolkit for accounting for allometry.

27 2. In this study, we used linear discriminant analysis to assess the discriminatory
28 performance of four published LMM protocols and a 3D GMM dataset for three clades of
29 antechinus known to differ subtly in shape. We assessed discrimination of raw data (which
30 are frequently used by taxonomists); data with isometry removed; and data after allometric
31 correction.

32 3. We found that group discrimination among raw data was high for LMM, possibly inflated
33 relative to GMM when visualised in PCA plots. However, GMM produced better results in
34 group discrimination after the size and allometry treatments. High measurement redundancy
35 in LMM protocols appears to result in relatively high allometry but low discriminatory
36 performance.

37 4. These findings suggest that taxonomic measurement protocols might benefit from GMM-
38 based pilot studies, because this offers the option of differentiating allometric and non-
39 allometric shape differences between species, which can then inform on the development
40 of the easier-to-apply LMM protocols.

- 41 **Keywords:** allometry – cryptic species – geometric morphometrics – linear discriminant
42 analysis – linear morphometrics – shape variation – taxonomy

43 **Introduction**

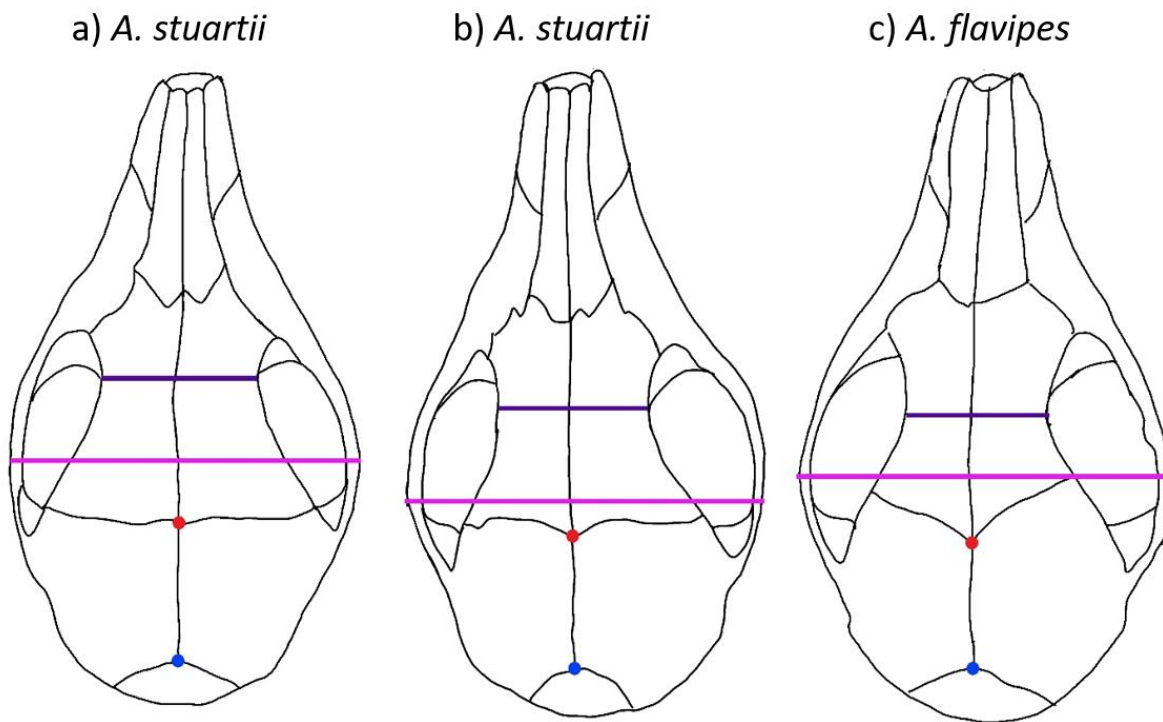
44 Morphometric measurements are an important tool in efforts to differentiate
45 mammalian species from each other, and have been used in taxonomic research for
46 centuries. Mammalian skulls in particular are widely used for taxonomic diagnostics and
47 have long provided important data which can be used in the delimitation of species or
48 Evolutionary Significant Units (ESUs). Cranial morphometric measurements are widely used
49 in the separation of closely related mammalian groups around the world, ranging across
50 disparate taxa such as rodents (Alhajeri, 2021), mustelids (Abramov et al., 2018; Gálvez-
51 López et al., 2022) and whales (Rosel et al., 2017).

52 Morphometrics-based taxonomic differentiation remains mostly the domain of linear
53 morphometrics (LMM) (Jackson & Groves, 2015), mainly because linear measurements are
54 easily taken and comparable to results from past studies. However, this approach has
55 several limitations. For example, taxonomists choose a set of linear distances based on their
56 expertise of the morphology of the taxon in question. This could pose a problem when these
57 linear protocols are not standardized among morphometricians, obtaining potentially
58 different acquisitions of data in studies of similar taxa but based on different protocols. In
59 addition, the linear distances measured in taxonomic diagnoses often include maximum and
60 minimum heights, widths and lengths that are easily identifiable to the eye. However, these
61 measurements may characterize conditions that are not necessarily biologically
62 homologous across taxa. This is because, when shapes differ, maximum or minimum
63 distances may not be comparable among individuals, as the point-to-point distance may
64 relate to different reference points that are not necessarily homologous (Figure 1).
65 Additionally, LMM describes the distance between two points, missing potentially relevant
66 variation between shapes and not retaining information about the original shape. Lastly, size

67 differences are not often accounted for in taxonomic studies using LMM, but there is a
68 problem of redundancy when linear measurements contain other linear measurements
69 within them (e.g., multiple measurements along the longitudinal axis of the skull). Similarly,
70 the frequent use of proportional ratios (e.g. skull length vs. width) is problematic because
71 many species display intraspecific allometry, such that genetically similar individuals will
72 differ in a ratio simply because they differ in size (Sidlauskas et al., 2011).

73 A potential refinement of LMM protocols could be offered by the use of Geometric
74 Morphometrics (GMM). GMM uses the coordinates of anatomical reference points as
75 identifiable shape variables in most or all the specimens in a given dataset. Since the 1990s,
76 this technique (Adams et al., 2004) has become the standard method for shape
77 characterization in evolutionary and ecological morphometrics and has a very mature
78 analytical toolkit (Fruciano, 2016; Fruciano et al., 2017). The holistic characterization of the
79 biological specimens under study and the graphical output of the associated shape changes
80 provide a powerful and alternative tool for biological inferences in many contexts
81 (Klingenberg, 2016; Stone, 1997), a definite advantage that linear morphometrics cannot
82 offer.

83



84

85 **Figure 1: Three specimens (CM12785, CM6540 and CM10548) outlining two commonly**
 86 **used linear distances: the width of greatest constriction of orbitotemporal fossa (dark**
 87 **purple) and the maximum width of cranium measured across zygomatic arches (pink).**
 88 **In addition, two type I homologous landmarks (by suture intersection) are depicted:**
 89 **the fronto-parietal suture in midline (red dot) an the parietal-interparietal suture in**
 90 **midline (blue dot). The two examples of maximum and minimum distances are**
 91 **measured at different anatomical positions relative to the homologous landmarks and**
 92 **other sutures in the skull, indicating a possibly serious lack of homology.**

93 GMM is rarely used in taxonomic studies, probably because linear measurements
 94 are easier to acquire and analyse, and because there is a large body of literature on
 95 taxonomic measurements that has been widely used for centuries (Sidlauskas et al., 2011).
 96 In addition, geometric morphometric data acquisition can be more complex, requiring
 97 digitisation of either photographs or 3D specimen representations, which generally involve
 98 specialized equipment. The statistical analyses required, while very well developed and
 99 versatile, are also specialised and involve high-dimensional data (Adams & Otárola-
 100 Castillo, 2013; Klingenberg, 2011; Zelditch et al., 2012). Therefore, they may not be
 101 perceived to be straightforward as the statistical toolkits used in LMM analyses.

102 We argue that GMM analyses are a useful addition to taxonomic studies because the
103 technique addresses several of the issues of LMM raised above. First, the analyses of the
104 main variation of a dataset based on a GMM protocol that optimizes anatomical coverage
105 could inform a LMM protocol to include linear distances with potential taxonomic
106 differentiators. Second, GMM can directly address primary homology by using fixed
107 homologous landmarks (e.g., suture intersections) and curve and surface semilandmarks
108 that correspond anatomically to each other (Gunz & Mitteroecker, 2013; Palci & Lee, 2019;
109 Zelditch et al., 2012). This contrasts to LMM, where often

110 measurements are chosen by the maximum and minimum distance from one point
111 to another regardless of whether they correspond anatomically. This LMM approach results
112 in distances potentially measured at different places relative to homologous reference points
113 such as tissue juxtapositions (Figure 1). Third, the distance between two points usually
114 measured in LMM protocols does not provide information on the geometry (i. e., curvature)
115 of the line drawn between them. GMM can use semilandmarks along curves or surfaces that
116 describe the shape between points in three dimensions, augmenting other potential
117 maximum or minimum distances to be taken into account in LMM protocols.

118 An additional advantage for GMM is the explicit treatment of size. The Procrustes
119 superimposition procedure inherent to GMM (Zelditch et al., 2012) allows the removal of the
120 size component from the dataset by scaling all specimens to the same size. This procedure
121 results in two components: a proxy for size called centroid size and a multivariate shape
122 component (Kendall, 1989). These can then be used for analyses of allometry (shape
123 changes disproportionate to size) in the form of a shape vs size regression (Klingenberg,
124 2016, 2022). This substantially improves on the issue of accounting for isometric and
125 allometric variation, which can have serious implications for taxon delimitation. Allometric

126 effects in particular can give an impression of species differentiation, when cranial allometry
127 is generally present within most mammalian species (Cardini et al., 2015; Marcy et al., 2020;
128 Viacava et al., 2020, 2021) and may not be related to morphological divergence due to a
129 speciation event (Sidlauskas et al., 2011). Such allometric variation has been regarded as
130 irrelevant to taxonomy. This is because, if shape differences were strictly due to size
131 differences, they are likely to be the differences between small and large animals within a
132 taxonomic group (Pilbeam & Gould, 1974; Seifert, 2008; Wood & Stack, 1980). In contrast,
133 non-allometric shape changes are thought to be caused by independent adaptive processes
134 such as are involved in species divergences (Huxley, 1931; Gould, 1975). Thus, it is
135 recommended to include allometric analyses in taxonomic studies in order to interpret the
136 shape variation and to properly delimit species (Cardini & Polly, 2013; Kaliontzopoulou et
137 al., 2008; Outomuro & Johansson, 2017; Seifert, 2008; Sidlauskas et al., 2011; Yazdi, 2014).
138 However, even in a case where taxonomic differentiation is driven purely by selection for
139 size and coincides only with allometry effects, this represents important information on the
140 differentiation process and should be considered.

141 Here, we compare the taxonomic differentiation performance of conventional, linear-
142 based morphometrics and 3D geometric morphometrics in a species complex that includes
143 three genetically differentiated taxonomic groups containing subtle morphological
144 differences (Viacava et al., 2021), the *A. stuartii* / *A. subtropicus* species complex. This
145 represents a scenario where finer-grained differences (e.g., allometric effects or differences
146 in non-homologous measurements) need to be identified and interpreted with great care to
147 understand their pertinence to group differentiation. The taxonomic situation of this species
148 complex is also useful because three linear morphometric protocols have been used
149 pertaining to the genus, allowing an assessment of how important protocol choice can be to
150 the delimitation of taxonomic units. We add to this also a more generic protocol developed

151 for bandicoots (Travouillon, 2016), with a particularly high number of linear measurements.
152 We use linear discriminant analysis to ask how well the four protocols and our GMM protocol
153 perform in a context typical to taxonomy (without consideration of size, or with consideration
154 only of isometry) and compare it to the analysis pipeline typically taken in GMM studies (with
155 allometric variation accounted for as well).

156 **Materials and methods**

157 All analyses are based on a 3D landmark coordinate dataset from Viacava et al.
158 (2021), which includes high-coverage 3D landmarked crania with 412 landmarks (82 fixed
159 landmarks, 185 curved semilandmarks and 145 surface semilandmarks) of 136 adult
160 individuals reconstructed in virtual 3D images. All analyses were performed in R version
161 4.0.4 (R Core Team, 2021). The code and raw 3D data are available on Github
162 (https://github.com/pietroviama/Viacavaetal_LMMvsGMM).

163 We identified four linear measurement protocols that represent traditional
164 morphometric methods commonly used in Australian mammal taxonomy, but are also
165 specific to *Antechinus*. These include a protocol used for a species contained in the species
166 complex studied here, *A. subtropicus* (Van Dyck & Crowther, 2000), a sister species of the
167 species complex studied here, *A. agilis* (Dickman et al., 1998), a species within the genus
168 *Antechinus*, *A. flavipes* (Baker & Van Dyck, 2013), and a comprehensive protocol that was
169 developed for Peramelemorphians (bandicoots) (Travouillon, 2016). The last protocol is not
170 necessarily expected to apply well to the genus *Antechinus* because it was designed for a
171 different order of marsupials. However, it was chosen as a useful comparison of
172 performance with the other three sets of linear measurements, representing one of the most

173 comprehensive protocols in the morphometric study of Australian mammals. All of these
174 protocols differ from each other, but overlap in some measurements (Table 1).

175

176

177 **Table 1. Degree of overlap of linear measurements between protocols. The LMM**
178 **protocols in the rows cover a fraction of the LMM protocols in the columns.**

	Van Dyck & Crowther, 2000	Dickman et al., 1998	Baker & Van Dyck, 2013	Travouillon, 2016
Van Dyck & Crowther, 2000		61.9 %	66.67 %	27.27 %
Dickman et al., 1998	100 %		72.22 %	40.91 %
Baker & Van Dyck, 2013	92.31 %	61.9 %		31.82 %
Travouillon, 2016	46.15 %	42.86 %	33.33 %	

179

180

181 To obtain linear measurement data, we extracted the linear distances of each
182 protocol that could be estimated most appropriately from the coordinates of the landmarks
183 used for the geometric morphometric approach (Supplementary Table S4.1). These
184 measurements were not exactly the same as calliper measurements; however, we assume
185 that slight inconsistencies between linear-based and 3D landmark-based distances are
186 acceptable because they were taken in a consistent fashion and the representation of shape
187 taken with the linear distances is not lost. We averaged right and left measurements
188 whenever possible.

189 *Isometry and allometry*

190 In geometric morphometrics, the isometric component of shape (i.e. the shape that
191 varies in a 1:1 proportion with size) is generally removed from the dataset through the scaling

192 procedure of the Procrustes superimposition. This step brings all specimens to the same
193 size, producing “isometry-free” shape coordinates and a centroid size (Dryden & Mardia,
194 2016; Klingenberg, 2016) for each specimen. Centroid size can be used subsequently as a
195 proxy for specimen size. To approximate this effect in the LMM context, we used an
196 approach that is analogous to centroid size extraction by deriving the geometric mean of all
197 variables as the centroid size, and using log-shape ratios [$\log_{10}(\text{measurement}/\text{geometric}$
198 $\text{mean})$] as isometry-free shape variables. This ensures that each dataset can be analysed
199 in an approximately equivalent way (Claude, 2013; Mosimann, 1970).

200 In order to assess the effect of allometry, we regressed the Procrustes shape
201 variation vs $\log(\text{centroid size})$ with the ‘geomorph’ (Adams & Otárola- Castillo, 2013)
202 function ‘procD.lm’. For LMM, we regressed the linear data vs $\log(\text{geometric mean})$ with the
203 *lm.rpp* function of the ‘RRPP’ package (Collyer & Adams, 2018). We considered both
204 centroid size and geometric mean as proxies for size in the context of geometric and linear
205 morphometrics. We also computed “allometry-free” datasets for the classification analyses
206 below, by using the residuals from the allometric regressions. In summary, three types of
207 morphological data were obtained and analysed for the LMM protocols and the GMM
208 dataset: a) raw 3D coordinates obtained from a partial Procrustes superimposition (GMM)
209 and raw linear measurements (LMM), b) shape after Procrustes superimposition (GMM) and
210 log-shape ratios as explained above (LMM), and c) allometry-corrected shape for both. In
211 the case of raw shape, this type of data is typically called “form” in geometric morphometrics
212 (shape plus size). However, for practical purposes, we will further call the types of
213 morphological data explained above as “raw”, “isometry-free” and “allometry-free” shape,
214 respectively. Allometric regressions were performed with 1000 permutations and p-values
215 were calculated using Goodall’s F-test (Goodall, 1991).

216 *Ordination*

217 To assess if the main variation of shape related to differentiation between species,
218 we computed Principal Component Analysis (PCA) for each treatment (raw, isometry-free
219 and allometry-free measurements) and each linear measurement protocol and geometric
220 morphometrics. However, note that lack of differentiation of groups in PC1/PC2 space does
221 not mean that the groups are not differentiated; PCA is agnostic to groupings, such that
222 variation that differentiates a particular group can also be “smeared” across many Principal
223 components (Bookstein, 2015, 2017a, 2017b; Klingenberg et al., 1996; Weisbecker et al.,
224 2019).

225 *Classification rule*

226 To assess how well specimens are predicted to belong to each group based on the
227 different analyses, we used 95% of the PC variance of each dataset to perform a Linear
228 Discriminant Analysis. We used the clade identity as a group factor and provided an equal
229 prior on class membership to the three groups. We plotted the two linear discriminants for
230 each treatment (raw, isometry-free and allometry-free measurements), and for each linear
231 measurement protocol and the geometric morphometrics protocol. Next, we used a machine
232 learning model known as leave-one-out cross validation procedure to calculate the posterior
233 probability values (Venables & Ripley, 2002). These values allowed us to use the ‘klaR’
234 package for R (Weihs et al., 2005) to calculate a number of metrics termed Garczarek’s
235 classification performance measures (Garczarek & Weihs, 2003), which include
236 Correctness Rate (CR), Accuracy (AC), Ability to Separate (AS), Confidence (CF), and
237 Confidence for each class. The CR and AC values estimate the degree of validity (“quality”)
238 of the linear discriminant analysis from the predicted values based on the true values. AS

239 corresponds to the distance between the posterior values and the assigned groups and CF
240 measures the degree of confidence to which the groups have been assigned – both AS and
241 CF estimate the “certainty” of the result of the linear discriminant analysis (Dr. Karsten
242 Luebke pers. comm.). Finally, we predicted the identity of unidentified specimens (n = 32).
243 For this, we predicted the PC scores of the unidentified specimens and then used the LDA
244 model of our “isometry-free” datasets to predict the class provenance for each specimen
245 (Supp. Table 1).

246 **Results**

247 *Allometry*

248 All LMM and GMM protocols were significantly allometric (Table 2). The amount of
249 shape variation attributable to allometry differed substantially, from 7.9% using Van Dyck &
250 Crowther’s linear measurement protocol, to over 25% using Travouillon’s linear
251 measurement protocol. Dickman et al., Baker & Van Dyck and GMM identified a similar
252 allometric effect of between 11 and 14% of shape variation explained by size (Table 2).

253 *Ordination*

254 The first Principal Component (PC1) of the three LMM protocols developed for
255 antechinuses accounted for more than 70% of morphological variation in raw, isometry-free
256 and allometry-free contexts (Figure 2). Travouillon et al.’s linear measurement protocol was
257 substantially affected in the amount of morphological variation accounted for by PC1 after
258 the removal of isometry, dropping from 73.36% to 38.33%, and to 24.65% after allometric
259 correction. We also observed a reduction in morphological variation accounted by PC1 after
260 removal of isometry in the GMM protocol, from 78.77% to 19.43%, and a slight decrease

261 after allometric correction to 14.78%. Grouping of the three clades was affected in all three
262 stages of data treatment; in all cases, isometry removal contributed to the assemblage of
263 the groups along PC1 and allometric correction scattered the three groups showing unclear
264 grouping (Figure 2).

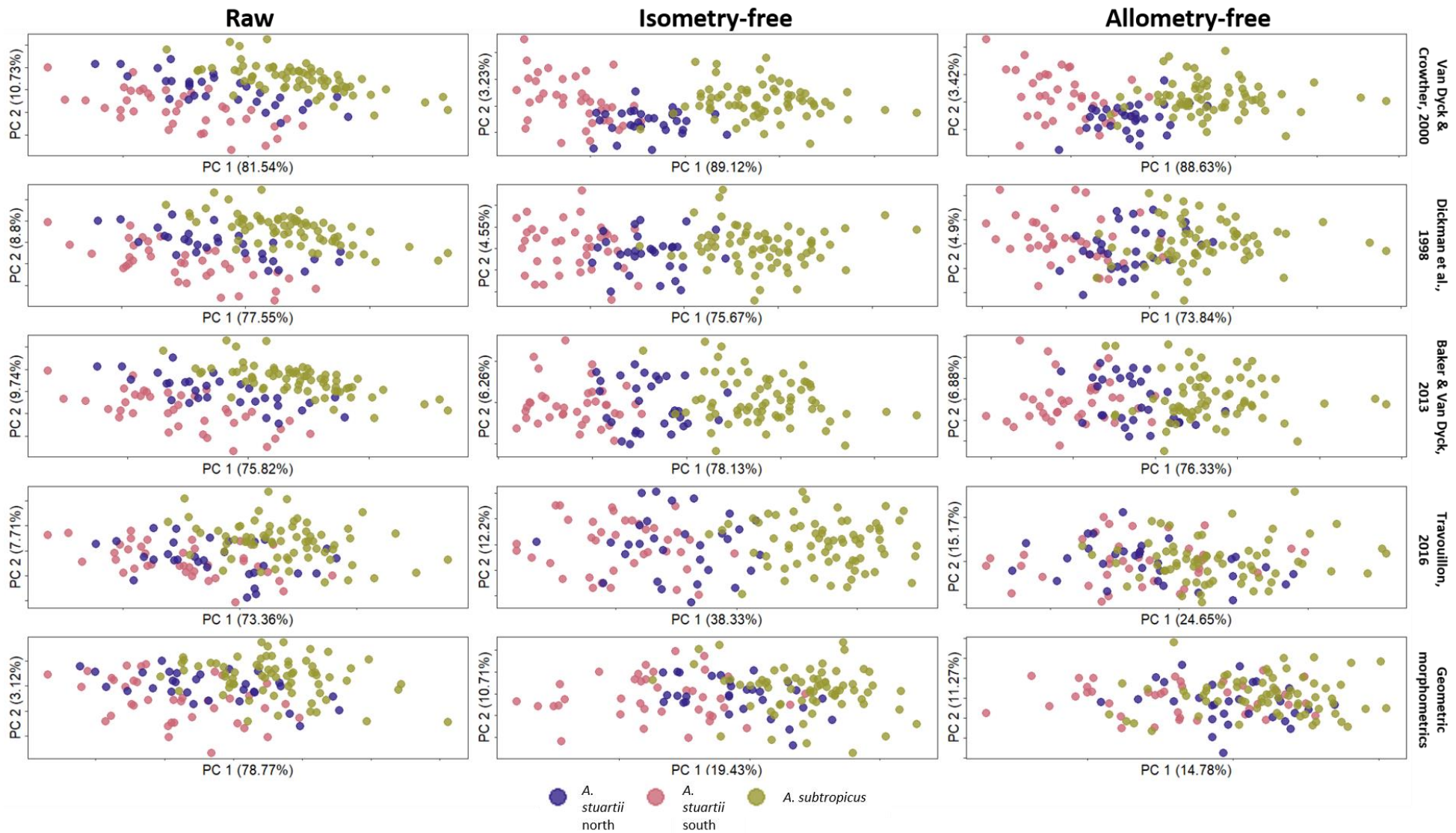
265 *Classification rule*

266 The Linear Discriminant Analysis plots display similar groupings of clades for raw and
267 isometry-free measurements. Interestingly, the removal of isometry increased group
268 differentiation in the GMM protocol, whereas the LMM protocols showed a considerable
269 decrease in group differentiation after removal of allometry (Figure 3 and Table 2). For GMM,
270 the removal of allometry did not affect group differentiation as much as for LMM (Figure 3
271 and Table 2).

272 For size-unadjusted raw data, the classification performance measures were
273 reasonably high in all four LMM protocols (Table 2). After isometry removal and allometric
274 correction, these measures decreased to varying degrees for all LMM protocols. GMM
275 performed better than LMM at group discrimination at the raw data stage. After the removal
276 of isometry, GMM performed similarly to LMM protocols in CR and AC (“quality” measures)
277 and better in AS and CF (“certainty” measures). After allometric correction, a large decrease
278 in CR and AC was observed in GMM data despite similar performance in AS and CF.

279 Class predictions for unidentified specimens are shown in Supp. Table 1.

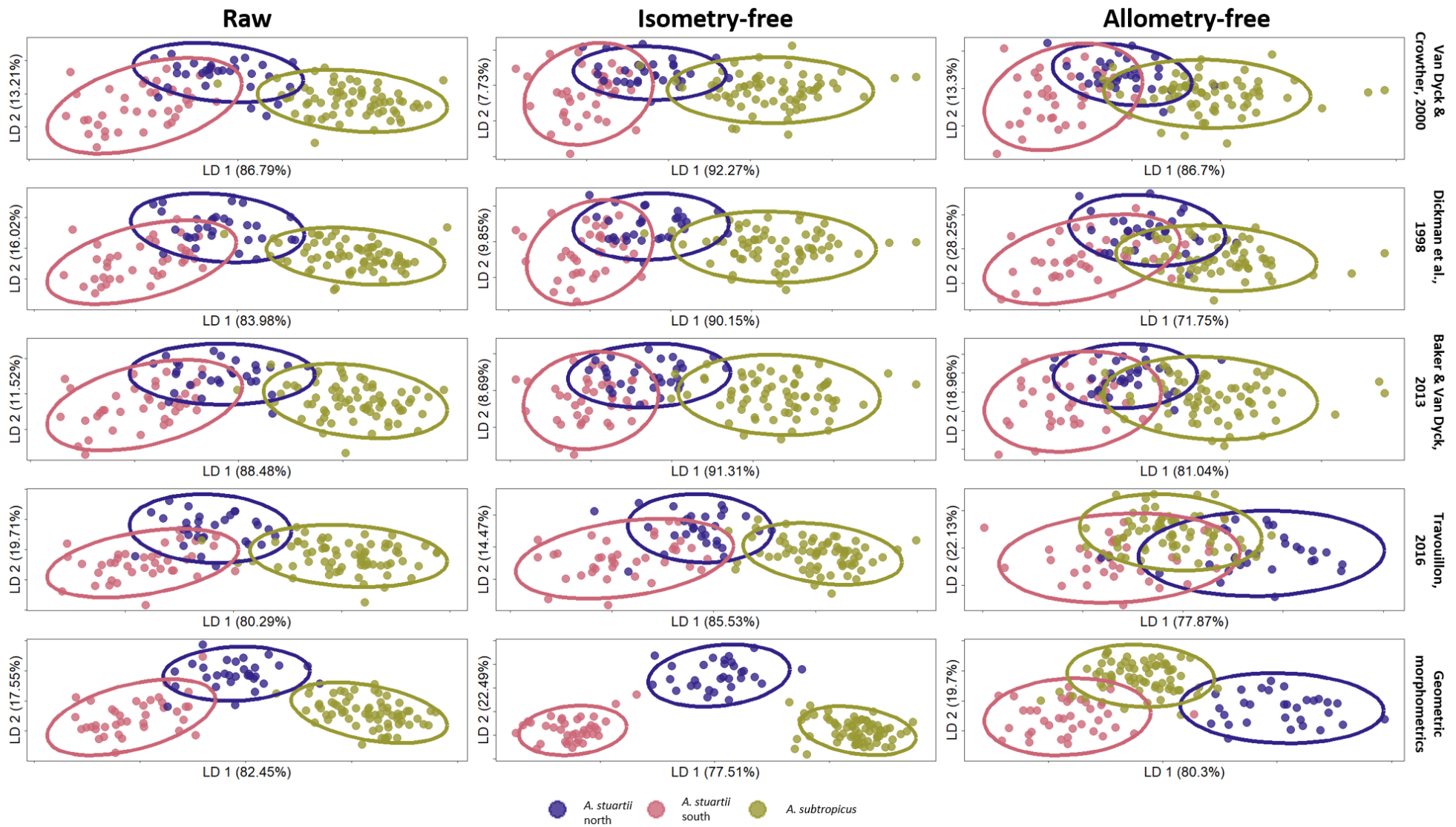
280



281

282
283

Figure 2: Principal Component Analyses plot for all raw, isometry-free and allometry-free datasets. These include the four linear measurement protocols and the geometric morphometrics approach. Only the first two Principal Components are shown.



284

285
286

Figure 3: Linear Discriminant Analyses plot for all raw, isometry-free and allometry-free datasets used in this study. These include the four linear measurement protocols and the geometric morphometrics approach. Ellipses were computed at 95% confidence intervals.

287
288
289

Table 2: Classification performance measures (Garczarek, 2002) of the four linear measurement protocols and geometric morphometrics. For each protocol, the classification performance measures were computed with raw datasets, after size treatment, and after allometry correction. Allometric regression results are also indicated in the last row.

	Van Dyck & Crowther, 2000			Dickman et al., 1998			Baker & Van Dyck, 2013			Travouillon, 2016			GMM		
	Raw	Isometry-free	Allometry-free	Raw	Isometry-free	Allometry-free	Raw	Isometry-free	Allometry-free	Raw	Isometry-free	Allometry-free	Raw	Isometry-free	Allometry-free
Correctness Rate	0.904	0.875	0.838	0.904	0.853	0.765	0.875	0.86	0.757	0.882	0.853	0.662	0.926	0.86	0.581
Accuracy	0.759	0.686	0.55	0.779	0.681	0.516	0.741	0.687	0.5	0.764	0.712	0.328	0.843	0.761	0.286
Ability to Separate	0.855	0.763	0.654	0.87	0.784	0.707	0.837	0.793	0.665	0.879	0.858	0.597	0.943	0.983	0.879
Confidence	0.915	0.861	0.79	0.924	0.874	0.817	0.905	0.879	0.794	0.927	0.914	0.749	0.967	0.99	0.928
Confidence for each true class	North: 0.89	North: 0.773	North: 0.72	North: 0.889	North: 0.802	North: 0.794	North: 0.86	North: 0.776	North: 0.726	North: 0.892	North: 0.863	North: 0.806	North: 0.963	North: 0.961	North: 0.947
	South: 0.875	South: 0.807	South: 0.787	South: 0.886	South: 0.817	South: 0.835	South: 0.87	South: 0.819	South: 0.783	South: 0.926	South: 0.897	South: 0.754	South: 0.953	South: 0.997	South: 0.944
	Sub: 0.949	Sub: 0.931	Sub: 0.823	Sub: 0.961	Sub: 0.937	Sub: 0.818	Sub: 0.945	Sub: 0.958	Sub: 0.83	Sub: 0.944	Sub: 0.946	Sub: 0.721	Sub: 0.976	Sub: 0.998	Sub: 0.91
Allometry	R ² = 0.079, F = 11.475, p = 0.001			R ² = 0.144, F = 22.48, p = 0.001			R ² = 0.113, F = 17.064, p = 0.001			R ² = 0.251, F = 44.99, p = 0.001			R ² = 0.132, F = 20.403, p = 0.001		

290

291 **Discussion**

292 Our results showed that linear morphometrics performed well in distinguishing
293 the three closely related species of antechinus in our dataset. However, the confidence
294 of differentiations was better for the geometric morphometric protocol, particularly after
295 size correction. There is also a clear indication that measurement choice has a
296 substantial influence on the discriminatory performance of a linear measurement
297 protocol.

298 We found that GMM performed relatively better at discriminating groups based
299 on raw and isometry-free data. However, the traditional morphometric protocols were
300 highly dependent on the choice of the measurements. The fewer variables relative to
301 GMM may therefore improve the discrimination of LMM protocols, but only if the
302 selected linear distances are the “real” best discriminatory ones. In the case of 3D
303 GMM, this dependence on measurement choice is expected to be less pronounced if
304 the creation of the landmarking template relies on the agnostic and comprehensive
305 placement of homologous reference points present in all specimens in a given dataset.
306 The selection of the landmarks should involve the construction of a template that
307 attempts the optimal anatomical coverage with diverse homologous points. This
308 process does not necessarily focus on the most variable regions because it can rely
309 on finding those differentiable shape patterns at the analytical step (Webster & Sheets,
310 2010). Thus, proportionally, some linear measurement protocols might be best at
311 discriminating but this will only be the case if the linear distances selected are best at
312 discriminating in “reality”. This is probably why the protocol developed for bandicoots
313 (Travouillon, 2016) had the lowest classification performance metrics among all

314 protocols (possibly exacerbated by the fact this was the only LMM protocol not
315 optimised for *Antechinus*).

316 Visual display of the main variation (PC1 vs PC2 plots; “PCA plots” from hereon
317 in) highlight the important issue that an interpretation solely based on the first principal
318 components can be misleading (Schreiber, 2021; Weisbecker et al., 2019) and in our
319 case can lead to a misunderstanding on the performance of GMM data. For GMM
320 data, the PCA plots revealed unclear grouping of the clades (see Figure 2), compared
321 to the much clearer differentiation of clades for the LMM protocols. However, the
322 classification performance measures that used 95% of PC variance of all protocols
323 reflect the ability of GMM to differentiate among clades exceedingly well (see Table
324 2).

325 This superficially better differentiation of the LMM PCA plots relative to the
326 GMM PCA plot is chiefly due to the lower dimensionality of the LMM dataset and the
327 fact that, in these particular cases, the linear distances chosen largely reflected the
328 differences among clades. However, this consideration can be deceptive given the low
329 variance explained by the first principal component in GMM, where in truth the
330 morphological variance tends to be distributed along a larger number of principal
331 components. This simply reflects the fact that the GMM dataset contains far more
332 variation overall, much of which does not differentiate clades. As PCA is agnostic to
333 group membership, this meant that the principal components containing variation that
334 discriminates groups were “hidden” in the lower ranks (Bookstein, 2017b; Klingenberg
335 et al., 1996; Weisbecker et al., 2019). The relevance of ignored morphological
336 variance in a PCA biplot in GMM is emphasized in our LDA results where 95% of the

337 PC variance was taken into account. This showed a more similar performance to group
338 discrimination in GMM and LMM relative to what we observed in the PCA plots.

339 The GMM protocol had an interesting property of numerically (and visually;
340 Figure 3) increasing the “certainty” measures of classification after the isometry
341 removal step (between raw and isometry-free datasets). The contribution of geometric
342 morphometrics towards isometry-free group separation may be a substantial
343 improvement in the way we regard size and shape as independent variables for
344 subsequent allometric analyses. In the case of geometric morphometrics, the large
345 number of landmarks may contribute to a holistic characterization of size – in the form
346 of centroid size (Mitteroecker & Gunz, 2009). In the LMM context, the linear distances
347 may contain fewer aspects of the size of the skull (Farkas et al., 2002; Slice, 2006).
348 For example, if we measured only the length or the width of a skull, other linear
349 distances associated with size-related shape could be ignored, such as the width of
350 the snout. This can be a problem because it disregards measures that are
351 characterizing the size of a three-dimensional object (Adams et al., 2004).
352 Furthermore, if size is not characterized well, further consequences on the
353 independence of a size and shape variable can undermine allometric analyses in the
354 form of a size vs shape regression (Klingenberg, 2016).

355 The removal of shape variation due to allometry (the step from “isometry-free”
356 to “allometry-free”) had a generally larger decrease in all classification performance
357 measures compared to the previous step of removal of isometry (from “raw” to
358 “isometry-free”). In the GMM dataset, this step of removal of allometry had a greater
359 decline in Correctness Rate and Accuracy but lesser decline in Ability to Separate and
360 Confidence (see Table 2) compared to the LMM protocols. This could be either

361 because of redundancy in the information of nearby landmarks and semilandmarks
362 resulting in “low quality” classification (low CR and AC), or because GMM deals more
363 effectively with allometric variation resulting in “highly certain” classification (highest
364 AS and CF among the datasets). We note that this result may be an indicator of the
365 former where the linear discriminant analysis may wrongly assign classes with false
366 “certainty” due to the poor ratio between variables (PC scores) and observations
367 (number of individuals) typically encountered in GMM. However, we suspect that the
368 latter is the case because the step of removal of allometry has a similar large decrease
369 on Accuracy in GMM and Travouillon’s protocol (2016), despite the particularly
370 stronger allometric relationship captured by Travouillon’s linear measurements. This
371 “large amount of allometry” captured by Travouillon may be caused by the redundancy
372 of some linear measurements that exacerbate some shape patterns driven by size.
373 However, if this was the case in GMM (i.e., high amount of allometry captured due to
374 redundant measurements), the Ability to Separate, reduced drastically in Travouillon,
375 should also be drastically reduced in GMM after removal of allometry. In contrast, what
376 we observe is high performance in Ability to Separate in GMM after the removal of
377 allometry. These contrasting results suggest that geometric morphometric techniques
378 provide a more thorough way of dealing with allometry-driven shape patterns
379 compared to linear measurements.

380 Our study suggests that GMM and its statistical toolkit provides improved
381 insights into taxon discrimination and particularly the influence of allometric patterns
382 that might not be taxonomically relevant. While GMM-based taxonomic studies are not
383 practical and are very time consuming, they are an excellent first “pilot” step to identify
384 linear measurements that are most likely to discriminate best within a group of interest.

385 Subsequently, linear morphometric studies can rely on the measurements that
386 account for the relevant shape patterns identified in GMM and be applied to larger
387 sample sizes.

388 Our results also highlight the dangers of introducing artificial group separation
389 due to “splitting” differently sized, but allometrically uniform taxonomic units. This is
390 not to say that size cannot be a distinguishing feature of two real taxonomic groups;
391 rather, understanding when variation relates to size, as opposed to other factors, can
392 help clarify the distinction between taxa as part of a wider discrimination toolkit (such
393 as genetics, pelage or behavioural traits).

394

395 **Acknowledgments**

396 We thank all museum collection curators who granted us access to scan the
397 specimens in their care: Heather Janetzki (Queensland Museum), Sandy Ingleby
398 (Australian Museum) and Christopher Wilson and Leo Joseph (Australian National
399 Wildlife Collection from the Commonwealth Scientific and Industrial Research
400 Organisation). We also thank P. V.’s Ph. D. thesis examiners Bastien Mennecart and
401 Laura Wilson for providing generous feedback, and finally Meg Martin for help in the
402 making of Figure 1.

403 P. V. was supported by a University of Queensland Research Training Tuition
404 Scholarship and a University of Queensland Research Higher Degree Living Stipend
405 Scholarship. This study was also financed by the Australian Research Council Future

406 Fellowship (FT180100634), Discovery Project (DP170103227) and Centre of
407 Excellence (CE170100015) awarded to V. W..

408

409 **Conflict of interest statement:** The authors declare no conflict of interest.

410 **Author's contribution statement:** P. V., V. W. and S. P. B. conceived the ideas and
411 designed methodology; P. V. collected the data; P. V. analysed the data; P. V. and V.
412 W. led the writing of the manuscript. All authors contributed critically to the drafts and
413 gave final approval for publication.

414 **Data accessibility statement:** All data and coded analyses are available in Github
415 (https://github.com/pietroviama/Viacavaetal_LMMvsGMM).

416

417 **References**

418 Abramov, A. V., Puzachenko, A. Y., & Masuda, R. (2018). Cranial Variation in the
419 Siberian Weasel *Mustela sibirica* (Carnivora, Mustelidae) and its Possible
420 Taxonomic Implications. *Zoological Studies*, 57, e14.
421 <https://doi.org/10.6620/ZS.2018.57-14>

422 Adams, D. C., & Otárola-Castillo, E. (2013). geomorph: An R package for the collection
423 and analysis of geometric morphometric shape data. *Methods in Ecology and*
424 *Evolution*, 4(4), 393–399.

- 425 Adams, D. C., Rohlf, F. J., & Slice, D. E. (2004). Geometric morphometrics: Ten years
426 of progress following the 'revolution.' *Italian Journal of Zoology*, 71(1), 5–16.
427 <https://doi.org/10.1080/11250000409356545>
- 428 Alhajeri, B. H. (2021). A morphometric comparison of the cranial shapes of Asian dwarf
429 hamsters (*Phodopus*, Cricetinae, Rodentia). *Zoologischer Anzeiger*, 292, 184–
430 196. <https://doi.org/10.1016/j.jcz.2021.04.001>
- 431 Baker, A. M., & Van Dyck, S. (2013). Taxonomy and redescription of the Yellow-footed
432 Antechinus , *Antechinus flavipes* (Waterhouse) (Marsupialia: Dasyuridae).
433 *Zootaxa*, 3649(1), 1–62. <https://doi.org/10.11646/zootaxa.3649.1>.
- 434 Bookstein, F. L. (2015). The Relation Between Geometric Morphometrics and
435 Functional Morphology, as Explored by Procrustes Interpretation of Individual
436 Shape Measures Pertinent to Function. *The Anatomical Record*, 298(1), 314–
437 327. <https://doi.org/10.1002/ar.23063>
- 438 Bookstein, F. L. (2017a). A method of factor analysis for shape coordinates. *American*
439 *Journal of Physical Anthropology*, 164(2), 221–245.
440 <https://doi.org/10.1002/ajpa.23277>
- 441 Bookstein, F. L. (2017b). A Newly Noticed Formula Enforces Fundamental Limits on
442 Geometric Morphometric Analyses. *Evolutionary Biology*, 44(4), 522–541.
443 <https://doi.org/10.1007/s11692-017-9424-9>
- 444 Cardini, A., & Polly, P. D. (2013). Larger mammals have longer faces because of size-
445 related constraints on skull form. *Nature Communications*, 4, 2458.

446 <https://doi.org/10.1038/ncomms3458>
447 <https://www.nature.com/articles/ncomms3458#supplementary-information>

448 Cardini, A., Polly, P. D., Dawson, R., & Milne, N. (2015). Why the long face?
449 Kangaroos and wallabies follow the same 'rule' of Cranial Evolutionary
450 Allometry (CREA) as Placentals. *Evolutionary Biology*, 42(2), 169–176.
451 <https://doi.org/10.1007/s11692-015-9308-9>

452 Claude, J. (2013). Log-shape ratios, Procrustes superimposition, elliptic Fourier
453 analysis: Three worked examples in R. *Virtual Morphology and Evolutionary*
454 *Morphometrics in the New Millenium.*, 94.

455 Collyer, M. L., & Adams, D. C. (2018). RRPP: An r package for fitting linear models to
456 high-dimensional data using residual randomization. *Methods in Ecology and*
457 *Evolution*, 9(7), 1772–1779.

458 Dickman, C. R., Parnaby, H. E., Crowther, M. S., & King, D. H. (1998). *Antechinus*
459 *agilis* (Marsupialia: Dasyuridae), a new species from the *A. stuartii* complex in
460 south-eastern Australia. *Australian Journal of Zoology*, 46(1), 1–26.
461 <https://doi.org/10.1071/zo97036>

462 Dryden, I. L., & Mardia, K. V. (2016). *Statistical shape analysis: With applications in R*
463 (Vol. 995). John Wiley & Sons.

464 Farkas, L. G., Tompson, B. D., Katic, M. J., & Forrest, C. R. (2002). Differences
465 Between Direct (Anthropometric) and Indirect (Cephalometric) Measurements
466 of the Skull. *Journal of Craniofacial Surgery*, 13(1), 105–108.

- 467 Fruciano, C. (2016). Measurement error in geometric morphometrics. *Development*
468 *Genes and Evolution*, 226(3), 139–158. <https://doi.org/10.1007/s00427-016->
469 0537-4
- 470 Fruciano, C., Celik, M. A., Butler, K., Dooley, T., Weisbecker, V., & Phillips, M. J.
471 (2017). Sharing is caring? Measurement error and the issues arising from
472 combining 3D morphometric datasets. *Ecology and Evolution*, 7(17), 7034–
473 7046. <https://doi.org/10.1002/ece3.3256>
- 474 Gálvez-López, E., Kilbourne, B., & Cox, P. G. (2022). Cranial shape variation in mink:
475 Separating two highly similar species. *Journal of Anatomy*, 240(2), 210–225.
476 <https://doi.org/10.1111/joa.13554>
- 477 Garczarek, U., & Weihs, G. (2003). Standardizing the Comparison of Partitions.
478 *Computational Statistics*, 18(1), 143–162.
479 <https://doi.org/10.1007/s001800300136>
- 480 Goodall, C. (1991). Procrustes methods in the statistical analysis of shape. *Journal of*
481 *the Royal Statistical Society: Series B (Methodological)*, 53(2), 285–321.
- 482 Gunz, P., & Mitteroecker, P. (2013). Semilandmarks: A method for quantifying curves
483 and surfaces. *Hystrix, the Italian Journal of Mammalogy*, 24(1).
484 <https://doi.org/10.4404/hystrix-24.1-6292>
- 485 Jackson, S., & Groves, C. (2015). *Taxonomy of Australian Mammals*. CSIRO
486 Publishing.

- 487 Kaliontzopoulou, A., Carretero, M. A., & Llorente, G. A. (2008). Head shape allometry
488 and proximate causes of head sexual dimorphism in *Podarcis* lizards: Joining
489 linear and geometric morphometrics. *Biological Journal of the Linnean Society*,
490 93(1), 111–124. <https://doi.org/10.1111/j.1095-8312.2007.00921.x>
- 491 Kendall, D. G. (1989). A survey of the statistical Theory of shape. *Statistical Science*,
492 4(2), 87–99. JSTOR.
- 493 Klingenberg, C. P. (2011). MorphoJ: an integrated software package for geometric
494 morphometrics. *Molecular Ecology Resources*, 11(2), 353–357.
- 495 Klingenberg, C. P. (2016). Size, shape, and form: Concepts of allometry in geometric
496 morphometrics. *Development Genes and Evolution*, 226(3), 113–137.
497 <https://doi.org/10.1007/s00427-016-0539-2>
- 498 Klingenberg, C. P. (2022). Methods for studying allometry in geometric
499 morphometrics: A comparison of performance. *Evolutionary Ecology*.
500 <https://doi.org/10.1007/s10682-022-10170-z>
- 501 Klingenberg, C. P., Neuenschwander, B. E., & Flury, B. D. (1996). Ontogeny and
502 Individual Variation: Analysis of Patterned Covariance Matrices with Common
503 Principal Components. *Systematic Biology*, 45(2), 135–150.
504 <https://doi.org/10.1093/sysbio/45.2.135>
- 505 Marcy, A. E., Guillerme, T., Sherratt, E., Rowe, K. C., Phillips, M. J., & Weisbecker, V.
506 (2020). Australian Rodents Reveal Conserved Cranial Evolutionary Allometry
507 across 10 Million Years of Murid Evolution. *The American Naturalist*, 196(6),
508 755–768. <https://doi.org/10.1086/711398>

509 Mitteroecker, P., & Gunz, P. (2009). Advances in geometric morphometrics.
510 *Evolutionary Biology*, 36(2), 235–247. <https://doi.org/10.1007/s11692-009->
511 9055-x

512 Mosimann, J. E. (1970). Size allometry: Size and shape variables with
513 characterizations of the lognormal and generalized gamma distributions.
514 *Journal of the American Statistical Association*, 65(330), 930–945.

515 Outomuro, D., & Johansson, F. (2017). A potential pitfall in studies of biological shape:
516 Does size matter? *Journal of Animal Ecology*, 86(6), 1447–1457.
517 <https://doi.org/10.1111/1365-2656.12732>

518 Palci, A., & Lee, M. S. Y. (2019). Geometric morphometrics, homology and cladistics:
519 Review and recommendations. *Cladistics*, 35(2), 230–242.
520 <https://doi.org/10.1111/cla.12340>

521 Pilbeam, D., & Gould, S. J. (1974). Size and Scaling in Human Evolution. *Science*,
522 186(4167), 892–901. <https://doi.org/10.1126/science.186.4167.892>

523 R Core Team. (2021). *R: A language and environment for statistical computing*. R
524 *Foundation for Statistical Computing, Vienna, Austria*.

525 Rosel, P. E., Taylor, B. L., Hancock-Hanser, B. L., Morin, P. A., Archer, F. I., Lang, A.
526 R., Mesnick, S. L., Pease, V. L., Perrin, W. F., Robertson, K. M., Leslie, M. S.,
527 Berta, A., Cipriano, F., Parsons, K. M., Viricel, A., Vollmer, N. L., & Martien, K.
528 K. (2017). A review of molecular genetic markers and analytical approaches
529 that have been used for delimiting marine mammal subspecies and species.
530 *Marine Mammal Science*, 33(S1), 56–75. <https://doi.org/10.1111/mms.12412>

- 531 Schreiber, J. B. (2021). Issues and recommendations for exploratory factor analysis
532 and principal component analysis. *Research in Social and Administrative*
533 *Pharmacy, 17*(5), 1004–1011. <https://doi.org/10.1016/j.sapharm.2020.07.027>
- 534 Seifert, B. (2008). Removal of allometric variance improves species separation in
535 multi-character discriminant functions when species are strongly allometric and
536 exposes diagnostic characters. *Myrmecological News, 11*, 91–105.
- 537 Sidlauskas, B. L., Mol, J. H., & Vari, R. P. (2011). Dealing with allometry in linear and
538 geometric morphometrics: A taxonomic case study in the *Leporinus*
539 *cylindriformis* group (Characiformes: Anostomidae) with description of a new
540 species from Suriname. *Zoological Journal of the Linnean Society, 162*(1), 103–
541 130. <https://doi.org/10.1111/j.1096-3642.2010.00677.x>
- 542 Slice, D. E. (2006). *Modern morphometrics in physical anthropology*. Springer Science
543 & Business Media.
- 544 Stone, J. R. (1997). The spirit of D'Arcy Thompson dwells in empirical morphospace.
545 *Mathematical Biosciences, 142*(1), 13–30. [https://doi.org/10.1016/S0025-](https://doi.org/10.1016/S0025-5564(96)00186-1)
546 [5564\(96\)00186-1](https://doi.org/10.1016/S0025-5564(96)00186-1)
- 547 Travouillon, K. J. (2016). Investigating dental variation in *Perameles nasuta* Geoffroy,
548 1804, with morphological evidence to raise *P. nasuta pallescens* Thomas, 1923
549 to species rank. *Zootaxa, 4114*(4), 351–392.
- 550 Van Dyck, S., & Crowther, M. S. (2000). Reassessment of northern representatives of
551 the *Antechinus stuartii* complex (Marsupialia: Dasyuridae): *A subtropicus* sp.

552 Nov. And *A. adustus* new status. *Memoirs-Queensland Museum*, 45(2), 611–
553 635.

554 Venables, W. N., & Ripley, B. D. (2002). *Modern Applied Statistics with S*. Springer
555 New York. <https://doi.org/10.1007/978-0-387-21706-2>

556 Viacava, P., Baker, A. M., Blomberg, S. P., Phillips, M. J., & Weisbecker, V. (2021).
557 Using 3D geometric morphometrics to aid taxonomic and ecological
558 understanding of a recent speciation event within a small Australian marsupial
559 (*Antechinus*: Dasyuridae). *Zoological Journal of the Linnean Society*, zlab048.
560 <https://doi.org/10.1093/zoolinlean/zlab048>

561 Viacava, P., Blomberg, S. P., Sansalone, G., Phillips, M. J., Guillerme, T., Cameron,
562 S. F., Wilson, R. S., & Weisbecker, V. (2020). Skull shape of a widely
563 distributed, endangered marsupial reveals little evidence of local adaptation
564 between fragmented populations. *Ecology and Evolution*, 10(18), 9707–9720.
565 <https://doi.org/10.1002/ece3.6593>

566 Webster, M., & Sheets, H. D. (2010). A Practical Introduction to Landmark-Based
567 Geometric Morphometrics. *The Paleontological Society Papers*, 16, 163–188.
568 <https://doi.org/10.1017/S1089332600001868>

569 Weihs, C., Ligges, U., Luebke, K., & Raabe, N. (2005). KfAR analyzing German
570 business cycles. In *Data analysis and decision support* (pp. 335–343). Springer.

571 Weisbecker, V., Guillerme, T., Speck, C., Sherratt, E., Abraha, H. M., Sharp, A. C.,
572 Terhune, C. E., Collins, S., Johnston, S., & Panagiotopoulou, O. (2019).
573 Individual variation of the masticatory system dominates 3D skull shape in the

574 herbivory-adapted marsupial wombats. *Frontiers in Zoology*, 16(1), 41.
575 <https://doi.org/10.1186/s12983-019-0338-5>

576 Wood, B. A., & Stack, C. G. (1980). Does allometry explain the differences between
577 “Gracile” and “Robust” australopithecines? *American Journal of Physical*
578 *Anthropology*, 52(1), 55–62. <https://doi.org/10.1002/ajpa.1330520108>

579 Yazdi, A. B. (2014). Application of geometric morphometrics to analyse allometry in
580 two species of the genus *Myrmica* (Hymenoptera: Formicidae). *Soil Organisms*,
581 86(1), 77–84.

582 Zelditch, M. L., Swiderski, D. L., & Sheets, H. D. (2012). *Geometric Morphometrics for*
583 *Biologists: A Primer*. Academic Press.

584

585

586

587

588

589

590

592 **Supp. Table 1:** Class predictions for unidentified specimens using isometry-free data.

	Van Dyck & Crowther, 2000		Dickman et al., 1998		Baker & Van Dyck, 2013		Travouillon, 2016		Geometric morphometrics	
	Class	Posterior probability (%)	Class	Posterior probability (%)	Class	Posterior probability (%)	Class	Posterior probability (%)	Class	Posterior probability (%)
CM12785	<i>A. subtropicus</i>	99.87	<i>A. subtropicus</i>	99.9	<i>A. subtropicus</i>	99.66	<i>A. subtropicus</i>	99.81	<i>A. stuartii south</i>	99.64
CM12786	<i>A. stuartii north</i>	84.95	<i>A. stuartii north</i>	81.17	<i>A. stuartii north</i>	88.92	<i>A. stuartii north</i>	90.51	<i>A. stuartii north</i>	100
JM21536	<i>A. stuartii north</i>	85.38	<i>A. stuartii north</i>	92.07	<i>A. stuartii north</i>	93.57	<i>A. stuartii south</i>	68.17	<i>A. stuartii south</i>	95.16
J3810	<i>A. stuartii south</i>	62.85	<i>A. stuartii north</i>	52.21	<i>A. stuartii north</i>	60.23	<i>A. stuartii north</i>	97.48	<i>A. stuartii north</i>	70.15
CM3795	<i>A. stuartii south</i>	87.99	<i>A. stuartii south</i>	94.54	<i>A. stuartii south</i>	89.58	<i>A. stuartii north</i>	67.2	<i>A. stuartii north</i>	100
J5030	<i>A. stuartii south</i>	93.87	<i>A. stuartii south</i>	93.94	<i>A. stuartii south</i>	91.17	<i>A. stuartii south</i>	86.6	<i>A. stuartii south</i>	100
JM4432	<i>A. stuartii north</i>	82.92	<i>A. stuartii north</i>	92.35	<i>A. stuartii north</i>	92.28	<i>A. stuartii north</i>	97.41	<i>A. stuartii north</i>	100
JM3944	<i>A. stuartii north</i>	92	<i>A. stuartii north</i>	98.69	<i>A. stuartii north</i>	93.86	<i>A. stuartii south</i>	90.03	<i>A. stuartii north</i>	100
M22782	<i>A. stuartii north</i>	88.39	<i>A. stuartii north</i>	96.85	<i>A. stuartii north</i>	93.28	<i>A. stuartii north</i>	98.8	<i>A. stuartii north</i>	100
M22784	<i>A. stuartii north</i>	93.36	<i>A. stuartii north</i>	90.94	<i>A. stuartii north</i>	95.2	<i>A. stuartii north</i>	99.72	<i>A. stuartii north</i>	99.99
M22785	<i>A. stuartii north</i>	58.88	<i>A. subtropicus</i>	51.36	<i>A. stuartii north</i>	57.38	<i>A. stuartii north</i>	88.51	<i>A. stuartii north</i>	100
J15888	<i>A. stuartii north</i>	51.45	<i>A. stuartii south</i>	51.48	<i>A. stuartii north</i>	59.4	<i>A. stuartii north</i>	91.51	<i>A. stuartii north</i>	100
JM14417	<i>A. stuartii north</i>	63.98	<i>A. stuartii north</i>	81.44	<i>A. stuartii north</i>	63.89	<i>A. subtropicus</i>	61.98	<i>A. stuartii north</i>	100
RT1	<i>A. stuartii north</i>	97.79	<i>A. stuartii north</i>	99.42	<i>A. stuartii north</i>	98.32	<i>A. stuartii north</i>	98.36	<i>A. stuartii north</i>	100
JM1600	<i>A. stuartii north</i>	80.24	<i>A. stuartii north</i>	81.09	<i>A. stuartii north</i>	83.52	<i>A. subtropicus</i>	69.26	<i>A. stuartii south</i>	96.95
JM1596	<i>A. stuartii north</i>	81.93	<i>A. stuartii north</i>	87.6	<i>A. stuartii north</i>	93.59	<i>A. stuartii north</i>	74.2	<i>A. stuartii north</i>	99.28

J17400	<i>A. subtropicus</i>	100								
J17401	<i>A. subtropicus</i>	82.82	<i>A. subtropicus</i>	83.59	<i>A. subtropicus</i>	97.78	<i>A. subtropicus</i>	93.8	<i>A. subtropicus</i>	100
J17402	<i>A. subtropicus</i>	100	<i>A. subtropicus</i>	100	<i>A. subtropicus</i>	100	<i>A. subtropicus</i>	99.97	<i>A. subtropicus</i>	99.49
J17403	<i>A. subtropicus</i>	99.97	<i>A. subtropicus</i>	99.99	<i>A. subtropicus</i>	99.99	<i>A. subtropicus</i>	99.96	<i>A. subtropicus</i>	100
J17406	<i>A. subtropicus</i>	99.38	<i>A. subtropicus</i>	99.72	<i>A. subtropicus</i>	99.9	<i>A. subtropicus</i>	86.44	<i>A. subtropicus</i>	100
JM1420	<i>A. stuartii north</i>	83.45	<i>A. stuartii north</i>	93.65	<i>A. stuartii north</i>	78.72	<i>A. stuartii north</i>	94.95	<i>A. stuartii north</i>	100
JM14415	<i>A. stuartii north</i>	79.26	<i>A. stuartii north</i>	86.65	<i>A. stuartii north</i>	88.53	<i>A. stuartii north</i>	64.21	<i>A. subtropicus</i>	99.84
J20265	<i>A. stuartii north</i>	95.54	<i>A. stuartii north</i>	96.88	<i>A. stuartii north</i>	97.77	<i>A. stuartii north</i>	72.12	<i>A. stuartii north</i>	93.19
MWA1	<i>A. stuartii north</i>	77.94	<i>A. stuartii north</i>	86.11	<i>A. stuartii north</i>	73.15	<i>A. stuartii north</i>	68.85	<i>A. stuartii north</i>	99.69
MWA2	<i>A. stuartii north</i>	81.1	<i>A. stuartii north</i>	83.42	<i>A. stuartii north</i>	78.38	<i>A. stuartii north</i>	98.39	<i>A. stuartii north</i>	100
CG1	<i>A. stuartii north</i>	88.79	<i>A. stuartii north</i>	76.56	<i>A. stuartii north</i>	88.12	<i>A. stuartii north</i>	75.14	<i>A. stuartii north</i>	100
JM20761	<i>A. stuartii north</i>	69.88	<i>A. stuartii north</i>	72.83	<i>A. stuartii north</i>	85.39	<i>A. stuartii north</i>	66.84	<i>A. stuartii north</i>	100
JM21357	<i>A. stuartii north</i>	83.37	<i>A. stuartii north</i>	85.79	<i>A. stuartii north</i>	88.05	<i>A. stuartii north</i>	96.27	<i>A. stuartii north</i>	100
JM14452	<i>A. subtropicus</i>	62.93	<i>A. stuartii north</i>	58.51	<i>A. stuartii north</i>	70.93	<i>A. subtropicus</i>	95.9	<i>A. stuartii north</i>	99.73
CM674	<i>A. subtropicus</i>	93.56	<i>A. subtropicus</i>	97.38	<i>A. subtropicus</i>	99.64	<i>A. subtropicus</i>	87.61	<i>A. subtropicus</i>	99.84
CM675	<i>A. stuartii north</i>	96.48	<i>A. stuartii north</i>	97.83	<i>A. stuartii north</i>	97.61	<i>A. stuartii north</i>	93.34	<i>A. subtropicus</i>	100